Measurement And Characterization of Radio Propagation Channels from The Patient Room Hub to The Nurse Station Server for WBAN Medical Applications

Achmad Mauludiyanto
Departement of Electrical Engineering
Institut Teknologi Sepuluh Nopember
Surabaya, Indonesia
maulud@ee.its.ac.id

Gamantyo Hendrantoro
Departement of Electrical Engineering
Institut Teknologi Sepuluh Nopember
Surabaya, Indonesia

Darien Raditya Krisdaniawan
Departement of Electrical Engineering
Institut Teknologi Sepuluh Nopember
Surabaya, Indonesia

Abstract — **As time passes, technology is demanded to be more sophisticated, efficient, and fully automatic. Technology development also impacts the medical field since hospitals require a tool that can automatically, thoroughly, and accurately record the physical condition of patients in the inpatient room and forward the results to be checked by the nurses on duty at the nurse station. Automation of patient data recording needs to be performed flexibly and comfortably for patients; thus, a wireless device channelling sensors on the patient's body to the nurse station is required. On this account, it demands a measurement to characterise the radio propagation channels. Therefore, this paper highlights the radio channel between the inpatient room hubs and the nurse station server. The measurement was performed in two rooms separated in the Antenna and Propagation Laboratory, representing an inpatient room and the nurse station. Further, the channel frequency was set at 3 GHz with a bandwidth of 200 MHz. The measuring instrument used is the Vector Network Analyzer (VNA). The results obtained in the form of radio channel parameters in the form of attenuation and time dispersion of the WBAN channel. The value of the channel response magnitude varies and is influenced by environmental factors in the room. The channel response phase that occurs in the WBAN channel is uniformly distributed. The recommended WBAN channel link is the BJ link with a channel response of -24.88807 dB, with point B as an inpatient room hub and point J as a nurse station server. The WBAN channel link that needs to be avoided is the BG link with a channel response of -50.71232 dB, with point B as an inpatient room hub and point G as a nurse station server.**

Keywords — *WBAN, Frequency Response, Impulse Response*

I. Introduction

Along with the development of telecommunication technology, technology is demanded to be more sophisticated, efficient, and fully automatic. Technology development also impacts the medical field since hospitals require a tool that can automatically, thoroughly, and accurately record the physical condition of patients in the inpatient room and forward the results to be checked by the nurses on duty at the nurse station. Automation of patient data recording needs to be performed flexibly and comfortably for patients; thus, a wireless device channelling sensors on the patient's body to the nurse station is required [1-2].

Considering the large number of patients being treated, a wireless network with a tree topology is needed which is centered on the server at the nurse station and branched out to the hub in each inpatient room to the sensors on the patient. To realize the network, it is necessary to know in advance the characteristics of the radio propagation channel used in order to design an appropriate digital communication system. Therefore, it requires measurement to characterise the radio propagation channels. In addition, this measurement aims to be able to design a good propagation channel in accordance with its purpose and function.

This paper discusses the results of measuring and characterising the radio channels between the inpatient room hub and the nurse station server. The measurement was executed in two rooms separated by a wall in the Antenna and Propagation Laboratory, namely B.305 and B.306. These rooms represented the inpatient room and the nurse station. Further, the channel frequency was set at 3 GHz with a bandwidth of 200 MHz [3]. This research employed two identical rectangular microstrip patch antennas with an operational frequency of 3 GHz. The channel response was identified by measuring the frequency response using the Vector Network Analyzer (VNA). The characterised channel parameters included attenuation and time dispersion. A frequency response chart was subsequently created to draw conclusions relevant to the designated objectives by employing the Cumulative Distribution Function technique. The novelty of this paper is to provide recommendations for WBAN radio channel model for the application of wireless communication systems between the inpatient room hub and the nurse station server.

II. Research Analysis

A. Wireless Body Area Network

Wireless Body Area Network (WBAN) refers to a developed network concept aiming to collect, process, and store the records of important physiological data on the human body through sensory media [2][4-7]. Those data are sent to the

How to cite: Mauludiyanto, A., Hendrantoro, G., & Krisdaniawan, D. R. (2022). Measurement And Characterization of Radio Propagation Channels from The Patient Room Hub to The Nurse Station Server for WBAN Medical Applications. *JAREE (Journal on Advanced Research in Electrical Engineering), 6*(2).

higher layer to be interpreted via wireless media. WBAN can be applied in various fields, such as health, military and defense, and entertainment [8-9]. WBAN applications can be found in the communication and entertainment industries, where WBAN must be capable of sending data with high data rates. In addition, WBAN must meet the following requirements [10]:
a. able to prioritise data transmission from more important sources or signals securely;
b. low power consumption and controlled transmit power;
c. possessing the operable and compatible capability in environments with numerous other wireless technologies.

In WBAN, it is crucial to identify the characters or characteristics of the adopted electromagnetic wave propagation, both in devices attached to the human body and those embedded in the human body. Based on the location of the sensor nodes on the WBAN channel, these nodes are classified into three types, namely:
a. Implant sensor nodes
    These nodes refer to a condition where the nodes are implanted in the human body. They are usually placed under the skin or in tissues in the human body.
b. Body surface sensor nodes
    These nodes refer to a condition where the nodes are attached to the surface of the human skin.
c. External nodes
    These nodes refer to a condition where the nodes do not come into contact with the human body.

The WBAN protocol helps medical personnel diagnose and treat patients quickly and accurately since it can be performed in real-time and remotely. WBAN is utilised for real-time monitoring; thus, it requires small latency and a high data rate. In ICUs, WBAN is applied by attaching it to the patients' bodies, and the placement of the sensor points on the patients' bodies can vary depending on the symptoms and treatment required.

B. Impulse Response

The impulse response refers to the channel transfer function in the time domain h(t). Usually, the impulse response is determined by employing the Inverse Fast Fourier Transformation method, converting from the channel transfer function in the frequency domain H(f). The impulse response can be modelled as a Time-Invariant Impulse Response since it is usually carried out on a fixed system. The impulse response *h(t)* of a Linear Time-Invariant (*LTI*) system is defined as the response from the system when the input is *δ(t)*, where [11]:

$$h(t) = T[\delta(t)] \tag{1}$$

If $h(t) = 0$ for $t < 0$, then the system can be regarded as a causal system.
Where :
h(t) : impulse response
δ(t) : input system
T : Linier Time-Invariant system

C. Frequency Response

If applying the convolution theorem of Fourier transform in a Linear Time-Invariant system, the formula is as follows [11-12]:

$$Y(\omega) = X(\omega)H(\omega) \tag{2}$$

where $X(\omega) = F[x(t)]$, $Y(\omega) = F[y(t)]$, $H(\omega)$ is the frequency response of the system, $F[x(t)] =$ Fourier transform of the input signal, and $F[y(t)] =$ Fourier transform of the output signal.

D. Radiation Pattern

The radiation pattern is defined as a graphical representation of the radiation characteristics of an antenna. The antenna's radiation pattern is referred to as the field pattern if it represents the field strength. In representing the radiation pattern graphically, the radiation pattern can be described in absolute or relative form. The relative form suggests a normalised radiation pattern, where each value of the radiation pattern is divided by its maximum value. The normalised radiation pattern thereby presents the following equation [13-15]:

$$F_{(\theta,\Phi)} = \frac{P_{(\theta,\Phi)}}{E_{(\theta,\Phi)max}} \tag{3}$$

Since the pointing vector only has a radiation component directly proportional to the square of the magnitude of the field strength, the power pattern expressed in the normalised pattern is equal to the square of the normalised field pattern.

$$P(\theta, \Phi) = \left|F^2_{(\theta,\Phi)}\right| \tag{4}$$

In general, the antenna radiation pattern is described in decibels. The decibel value of the field intensity is thereby obtained by the following equation:

$$F_{(\theta,\Phi)} = 20 \, log\left|F_{(\theta,\Phi)}\right| \tag{5}$$

Where :
$F_{(\theta,\Phi)}$: normalised field pattern
$P_{(\theta,\Phi)}$: normalised power pattern
$E_{(\theta,\Phi)max}$: maximum value of electric field

The radiation pattern consists of three parts: the main lobe, side lobe, and back lobe. The main lobe is a radiation area with the highest intensity. Meanwhile, the side lobe refers to a radiation area with a lower intensity than the main lobe, and the back lobe performs the opposite direction of radiation from the main lobe. The main lobe consists of Half-Power Beamwidth (HPBW) and Beamwidth Between First Null (BWFN). HPBW is the angle at which the radiation intensity is half (-3dB) of the highest intensity. Conversely, BWFN is the angle at which the radiation intensity reaches zero.

In identifying the radiation pattern, it is necessary to measure the distance, which is an essential factor. The farther the measurement distance, the better the measurement results. Since the measurement cannot be made at an infinite distance, the measurement is taken at a considerably far field.

Determining the far-field distance can be defined by adopting the following equation [13-15]:

$$r > \frac{2D^2}{\lambda} \quad with\ r\ "D\ and\ r"\ \lambda \tag{6}$$

Where :
r : measurement distance
D : length of the antenna
λ : emitted wavelength by the antenna

Based on the pattern, radiation is categorised into three types:

1. *Isotropic*
    The isotropic radiation pattern is defined as a radiation pattern that emits the same radiation intensity in all directions. The radiation pattern has a spherical shape (ball shape).
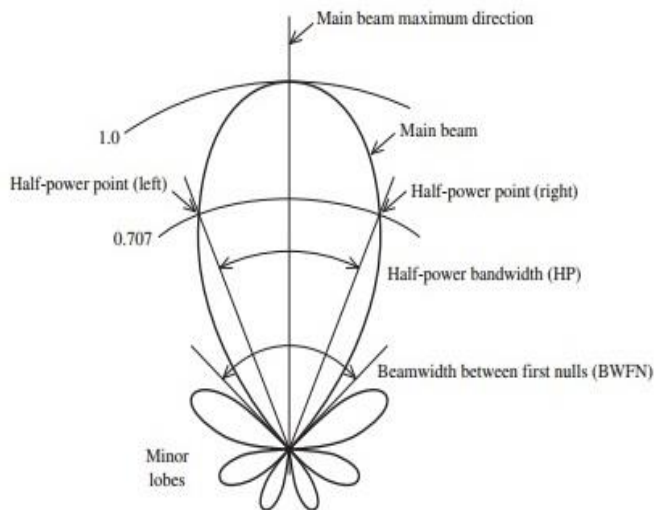

Fig. 1. Directional Antenna Radiation Pattern [15]

2. *Omnidirectional*
    The omnidirectional radiation pattern refers to a radiation pattern that emits radiation intensity in all directions.
3. *Directional*
    The directional radiation pattern refers to a radiation pattern that only emits radiation intensity in a specific direction. The directional radiation pattern can be observed in Fig. 1.

III. SIMULATION DESIGN AND DATA ANALYSIS

A. Measurement System

This study measured S21 parameters using Agilent N992A VNA and two identical rectangular microstrip patch antennas with a frequency of 3 GHz functioning as the transmitter and the receiver. The measurement was conducted in rooms B.305 and B.306 by setting five positions of antennas in room B.305 as the transmitters and six positions of antennas in room B.306 as the receivers. Following the antenna positions, each was paired with the other, resulting in a total of 30 antenna links. The plan of the Antenna and Propagation laboratory is illustrated in Fig. 2.

The two identical rectangular microstrip patch antennas were each connected to the VNA through the connector provided on the VNA. Port 1 of the VNA was connected to the rectangular microstrip patch antenna in room B.305 as the transmitter, while Port 2 of the VNA was connected to the rectangular microstrip patch antenna in room B.306 as the receiver. These links resulted in S21 parameters in the form of magnitude and phase. The magnitude and phase could be saved on a USB flash drive in an image and file format with the CSV file extension. The CSV files were subsequently exported and saved on a computer to be processed.
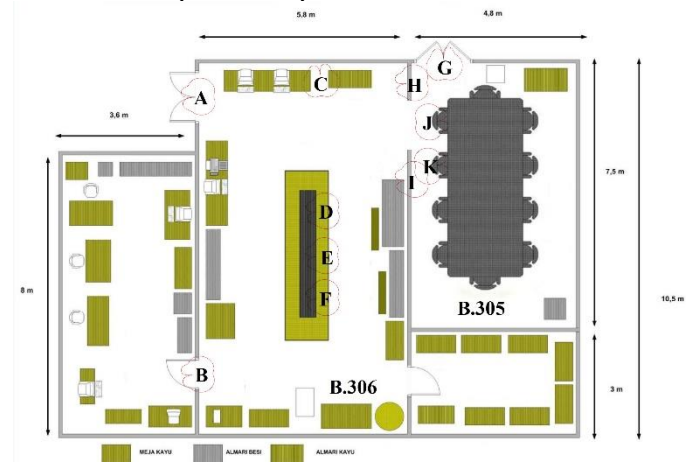

Fig. 2. Measurement Plan

B. Antenna Radiation Field

In this measurement, the antenna radiation field needed to be calculated to determine the antenna's far-field and near-field. This measurement adopted a microstrip patch antenna with a maximum dimension of 4.6 cm (0.046 m) and a wavelength of 0.1 m. Moreover, the following equation was employed to measure the antenna's far-field:

$$r > \frac{2D^2}{\lambda}$$

Thus, the far-field distance result was:

$$r > \frac{2(0,046)^2}{0,1}$$
$$r > 0.0423 \text{ m}$$
$$r > 4.23 \text{ cm}$$

Meanwhile, the following equation was employed to measure the near-field:

$$0.62\sqrt{\frac{D^3}{\lambda}} \le R \le 2\frac{D^2}{\lambda}$$

Thus, the near-field distance was:

$$0.62\sqrt{\frac{0,046^3}{0,1}} \le R \le 2\frac{0,046^2}{0,1}$$
$$0.0193 \text{ m} \le R \le 0.0423 \text{ m}$$
$$1.93 \text{ cm} \le R \le 4.23 \text{ cm}$$

Meanwhile, the relative near-field was calculated using the following equation:

$$R < 0.62\sqrt{\frac{D^3}{\lambda}}$$
$$R < 0.62\sqrt{\frac{0,046^3}{0,1}}$$
$$R < 0.0193 \text{ m}$$
$$R < 1.93 \text{ m}$$

C. Measurement Set-Up

This measurement included 11 antennas, precisely six antennas in room B.306 and five antennas in room B.305. In Fig. 2, the antennas in room B.306 are represented by points A, B, C, D, E, and F, while the antennas in room B.305 are represented by points G, H, I, J, and K. The antennas at points A and C are LOS propagation connected with room B.305. The antennas set at such positions usually have a high receiving power. The antenna at point B has a LOS link connected with point G. At points D, E, and F, the antennas are adjacent to each other at a certain distance. The antenna at point G is affected by external conditions. Further, the antennas at points H, I, and K have NLOS links connected with the antennas in room B.306. The antenna at point J has both LOS and NLOS links connected with several antennas in room B.306. Fig. 3 displays the antenna points set in room B.306. Room B.305 covers five antenna positions, i.e., points G, H, I, J, and K, as presented in Fig. 4.

The measurement generated the channel response magnitude data, which could be perceived from the S21 value in dB. The magnitudes obtained were subsequently reduced by the cable losses to determine the net values without the cable losses, which amounted to -27.66 dB. The numbers obtained were then multiplied by the square of the distance (r) to eliminate the existing distance effect. Next, these values were reduced by the antenna gain ($G_{antenna}$) of 2.36 dB to eliminate this element. Thus, the calculations resulted in several data, as displayed in Table I.

Fig. 3. Antennas in room B-306

Fig. 4. Antennas in room B-305

TABLE I. DATA RESULTING FROM CHANNEL RESPONSE MAGNITUDE MEASUREMENT

Link/Channel	r (m)	Link/Channel Condition	Measured S_{21} (dB)	Cable loss (dB)	GAntenna (dB)	Final S_{21} (dB)
AG	7.57	NLOS	-49.50380			-31.92188
AH	6.19	NLOS	-60.92065			-45.08684
AI	6.68	NLOS	-46.00697			-29.51144
AJ	8.41	LOS	-47.18799			-28.69207
AK	8.51	NLOS	-54.45394			-35.85535
BG	9.09	LOS	-69.88360			-50.71232
BH	10.26	NLOS	-51.69447			-31.47152
BI	7.95	NLOS	-48.07941			-30.07206
BJ	10.68	LOS	-45.45950			-24.88807
BK	10.3	NLOS	-48.25593			-27.99919
CG	3.9	NLOS	-51.15824			-39.33694
CH	2.6	NLOS	-46.23718			-37.93772
CI	4.38	NLOS	-50.82564			-37.99616
CJ	5.18	LOS	-52.29604			-38.00945
CK	5.4	NLOS	-53.42829			-38.78042
DG	7.94	LOS	-47.60101	-27.66	-2.36	-29.60460
DH	4.82	NLOS	-51.77052			-38.10958
DI	2.64	NLOS	-46.11579			-37.68371
DJ	5.34	LOS	-53.61554			-39.06471
DK	5.08	NLOS	-48.49704			-34.37914
EG	7.08	LOS	-53.33088			-36.33021
EH	5.68	NLOS	-58.37775			-43.29079
EI	3.14	NLOS	-50.15540			-40.21681
EJ	5.89	NLOS	-60.95095			-45.54865
EK	5.56	NLOS	-51.04873			-36.14723
FG	8.02	LOS	-50.29249			-32.20900
FH	6.68	NLOS	-61.62395			-45.12842
FI	3.92	NLOS	-46.26325			-34.39753
FJ	6.62	NLOS	-49.64215			-33.22499
FK	6.22	NLOS	-60.23273			-44.35692

D. Wave Propagation Mechanism

The measurement was conducted to identify the characteristics of the propagation channels. The measurement revealed that each of the 30 antenna links performed a mechanism similar to one another. These links consisted of 8 LOS links and 22 NLOS links. The LOS links included AJ, BG, BJ, CJ, DG, DJ, EG, and FG, while the rest were NLOS links. Some examples of LOS links can be previewed in Fig. 5.
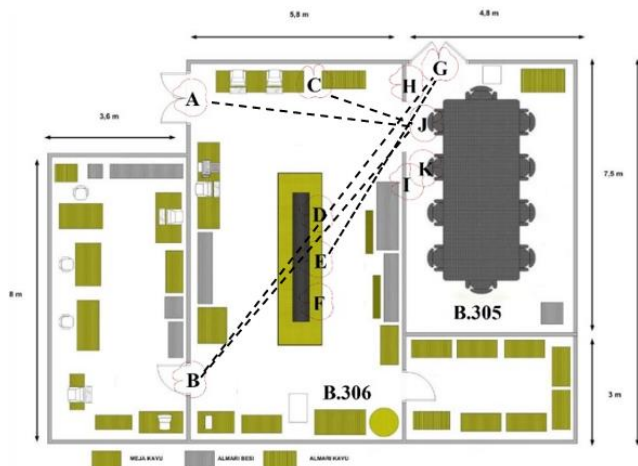

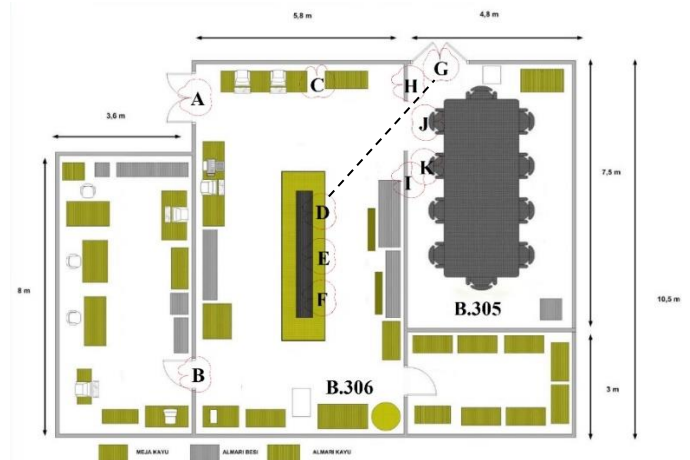Fig. 5. Several Examples of LOS Links

Fig. 6. DG Link

The wave propagation mechanisms consist of several stages, for example, the link between the antennas at point D and point G. As displayed in Fig. 6, points D and G were connected with a Line of Sight (LOS) propagation channel. Line of Sight is a condition where the propagation channel between the transmitter and receiver is unobstructed. In general, LOS propagation channels have a large receiving power. It is because the transmitter sends a signal straight to the receiver seamlessly. The amount of power received is also influenced by the antenna gain applied. In contrast, the link between points F and K, illustrated in Fig. 7, had a Non-Line of Sight (NLOS) propagation channel. Non-Line of Sight is a condition in which the propagation channel between the transmitter and receiver has a barrier or obstacle, resulting in a relatively small receiving power value. Besides the LOS and NLOS, the positioning of the antenna also affects the amount of power received. The greater the power received, the more accurate the data sent and vice versa.
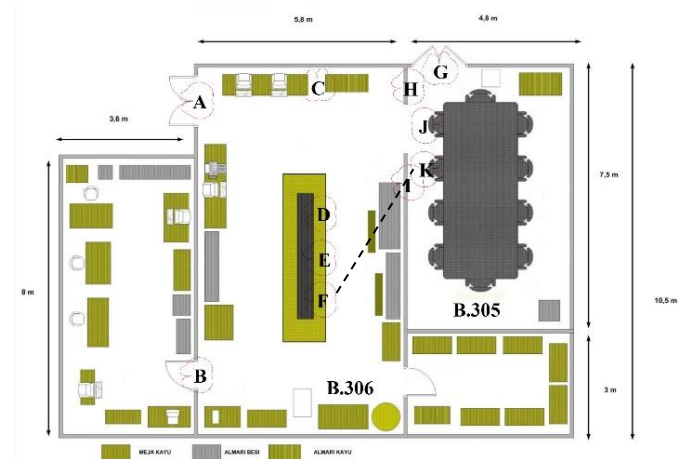

Fig. 7. FK link

The antenna links connecting points D, E, and F with the points G and J are presented in Fig. 8. In this case, the antenna at point D had a higher reception power than that at point E. Meanwhile, the antenna at point E had a higher reception power

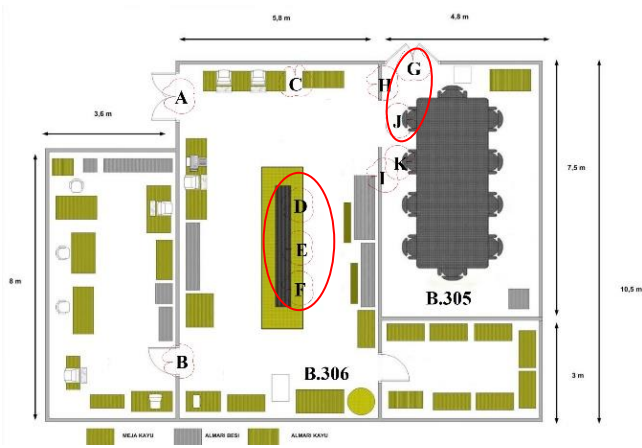than that at point F, even though there were some obstructions in the propagation channel.

Fig. 8. Antenna at Points D, E, F, G, J

The data collected was subsequently converted to Cumulative Distribution Function graphs to distinguish between the LOS and NLOS links. The graph of the Cumulative Distribution Function of magnitude was created based on the data in Table I, while the graph of the Cumulative Distribution Function of phase was created based on the data in Table II. The graphs of the Cumulative Distribution Function of magnitude and phase, respectively, can be observed in Fig. 9 and Fig. 10. By adopting the Cumulative Distribution Function, a similar step was also made on the phase value to examine the phase difference between when the link was in the LOS state and when the link was in the NLOS state.

TABLE II. Data on The Measurement Result of Channel Response Phase

Link/Channel	Link/Channel Condition	Channel Response Phase (degrees)
AG	NLOS	140.7849
AH	NLOS	9.72123
AI	NLOS	-98.00784
AJ	LOS	118.52199
AK	NLOS	-19.28853
BG	LOS	-33.03375
BH	NLOS	53.92190
BI	NLOS	56.06524
BJ	LOS	-18.35803
BK	NLOS	-63.34879
CG	NLOS	169.64961
CH	NLOS	-54.57134
CI	NLOS	-173.87948
CJ	LOS	60.90758
CK	NLOS	102.79350
DG	LOS	39.63551
DH	NLOS	-123.68523
DI	NLOS	7.63644

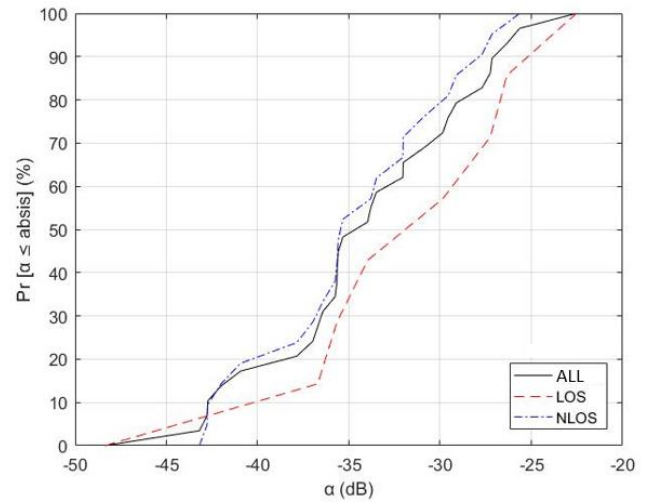|		
DJ	LOS	-122.54661
DK	NLOS	-124.73456
EG	LOS	-177.38302
EH	NLOS	61.91916
EI	NLOS	-76.08892
EJ	NLOS	69.05894
EK	NLOS	-77.07907
FG	LOS	-91.90158
FH	NLOS	-12.68159
FI	NLOS	71.90346
FJ	NLOS	83.50516
FK	NLOS	-127.38934

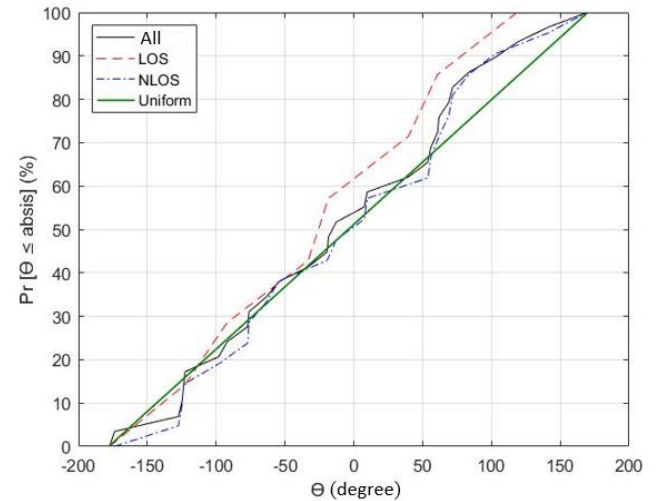Fig. 9. Graph of Cumulative Distribution Function of Magnitude

Fig. 10. Graph of Cumulative Distribution Function of Phase

IV. CONCLUSIONS AND SUGGESTIONS

By adopting a Vector Network Analyzer (VNA) measuring instrument, radio channel parameters in the forms of attenuation and time dispersion of the WBAN channel are measurable. The characteristics of a radio channel can be determined by taking

measurements using WBAN standard parameters and graphing the Cumulative Distribution Function.

The designed channel modelling had different magnitude values influenced by environmental factors, such as reflective objects that can increase multipath propagation. The channel response phase occurring in the WBAN channel was uniformly distributed.

The recommended WBAN channel link is the BJ link with a channel response of -24.88807 dB, with point B as an inpatient room hub and point J as a nurse station server.

The WBAN channel link that should be avoided is the BG link with a channel response of -50.71232 dB, with point B as an inpatient room hub and point G as a nurse station server.

Thus, it is crucial to determine the position of the inpatient room hub and nurse station server, both the distance and the link path that occurs between the inpatient room hub and the nurse station server.

ACKNOWLEDGMENT

REFERENCES

[1]   H. Viittala, M. Hamalainen, J. Iinatti and A. Taparugssanagorn, "Different Experimental WBAN Channel Models and IEEE802.15.6 Models: Comparison and Effects," *2009 2nd International Symposium on Applied Sciences in Biomedical and Communication Technologies*, Bratislava, 2009, pp. 1-5.

[2]   H. Sun, Z. Zhang, R. Q. Hu and Y. Qian, "Wearable Communications in 5G: Challenges and Enabling Technologies," in *IEEE Vehicular Technology Magazine*, vol. 13, no. 3, pp. 100-109, Sept. 2018.

[3]   K. P. Kartika, G. Hendrantoro, A. Mauludiyanto, "Pathloss Modelling Based on Measurement at 3GHz for on Body Area Network Application", 905-910. 10.1109/ICOIACT.2018.8350667. 2018.

[4]   M. Hämäläinen, A. Taparugssanagorn and J. Iinatti, "On the WBAN Radio Channel Modelling for Medical Applications," *Proceedings of the 5th European Conference on Antennas and Propagation (EUCAP)*, Rome, 2011, pp. 2967-2971.

[5]   V. Niemelä, M. Hämäläinen, J. Iinatti and A. Taparugssanagorn, "P-rake Receivers in Different Measured WBAN Hospital Channels," *2011 5th International Symposium on Medical Information and Communication Technology*, Montreux, 2011, pp. 42-46.

[6]   H. B. Lim, D. Baumann and E. Li, "A Human Body Model for Efficient Numerical Characterization of UWB Signal Propagation in Wireless Body Area Networks," in *IEEE Transactions on Biomedical Engineering*, vol. 58, no. 3, pp. 689-697, March 2011.

[7]   M. Ghamari, B. Janko, R. Sherratt, W. Harwin, R. Piechockic, and C. Soltanpur, "A Survey on Wireless Body Area Networks for eHealthcare Systems in Residential Environments," *Sensors*, vol. 16, no. 6, p. 831, Jun. 2016.

[8]   A. Pellegrini, A. Brizzi, L. Zhang, K. Ali, Y. Hao, X. Wu, C. C. Constantinou, Y. Nechayev, P. S. Hall, N. Chahat, M. Zhadobov dan R. Sauleau, "Antennas nad Propagation for Body-Centric Wireless Communication at Milimeter-Wave Frequencies," *IEEE Antennas Propagation Magazine,* vol. 55, no. 4, pp. 262-287, 2013.

[9]   D. B. Smith, D. Miniutti, T. A. Lamahewa dan L. W. Hanlen, "Propagation Models for Body-Area Networks:," *IEEE Antennas Propagation Magazine,* vol. 55, no. 5, pp. 97-117, 2013.

[10]   K. S. Kwak, S. Ullah and N. Ullah, "An overview of IEEE 802.15.6 standard," *2010 3rd International Symposium on Applied Sciences in Biomedical and Communication Technologies (ISABEL 2010)*, Rome, 2010, pp. 1-6.

[11]   I. C. Triaji, G. Hendrantoro, P. Handayani, "Statistik Respons Kanal Radio Dalam Ruang pada Frekuensi 2,6 GHz", Institut Teknologi Sepuluh Nopember, 2010.

[12]   Downey Allen B., "Think Stats, Second Edition", United States of America: O'Reilly Media, Inc. 2014.

[13]   Rasyidin Nazmi, Hendrantoro Gamantyo, Setijadi Eko, "Rancang Bangun Antena Microstrip Array untuk Sistem Radar Berbasis *Software Defined Radio*", Institut Teknologi Sepuluh Nopember, 2016.

[14]   Ludwig Reinhold, Bretchko Pavel "RF Circuit Design Theory and Application", Prentice-Hall, Inc., 2000.

[15]   Stutzman Warren L., Thiele Gary A., "Antenna Theory and Design, Third Edition", Wiley, 2012.